

Anomalous elastic hardening in Fe-Co alloys at high temperature

Hualei Zhang,^{1,2,*} Xiaoqing Li,² Stephan Schönecker,² Henrik Jespersen,³ Börje Johansson,^{2,4} and Levente Vitos^{2,4,5,*}

¹Center of Microstructure Science, Frontier Institute of Science and Technology, Xi'an Jiaotong University, Xi'an, 710054, China

²Applied Materials Physics, Department of Materials Science and Engineering, Royal Institute of Technology, Stockholm SE-100 44, Sweden

³Uddeholms AB, SE-683 85 Hagfors, Sweden

⁴Department of Physics and Astronomy, Division of Materials Theory, Uppsala University, Box 516, SE-75120, Uppsala, Sweden

⁵Wigner Research Center for Physics, Research Institute for Solid State Physics and Optics, Budapest H-1525, P.O. Box 49, Hungary

(Received 4 March 2014; revised manuscript received 13 March 2014; published 12 May 2014)

The elastic moduli of $\text{Fe}_{1-c}\text{Co}_c$ ($c \leq 0.2$) alloys are found to decrease strongly with increasing temperature, but show very weak alloying effects for both low-temperature ferromagnetic and high-temperature paramagnetic states. For temperatures slightly below and around the Curie temperature of Fe, Co addition significantly increases the elastic moduli. The variation of the tetragonal shear elastic constant upon 20% Co addition increases from a small negative value to more than 135% as the temperature rises from 0 to 1200 K. The expected elastic softening in the case of Al doping is not confirmed. Both anomalous trends are ascribed to the interplay between intrinsic chemical effects, magnetism, and temperature.

DOI: 10.1103/PhysRevB.89.184107

PACS number(s): 62.20.de, 71.15.Nc, 75.50.Bb

The great variety of properties Fe and its alloys exhibit is due to magnetism, which at low temperatures stabilizes the body centered cubic (bcc) phase instead of the hexagonal structure as predicted for nonmagnetic transition metals [1]. Increasing temperature destroys the magnetic long-range order, leading first to the correlated [2] paramagnetic bcc phase between 1043 and 1183 K and then to the less correlated [3] paramagnetic face centered cubic phase up to 1667 K. Iron melts at 1811 K from the bcc phase. Any mechanism that alters the magnetic interaction in Fe is expected to have a sizable impact on the fundamental thermophysical properties.

Cobalt is a common alloying element in Fe-based steels. The Fe-rich Fe-Co alloys exhibit high Curie temperature, high saturation magnetization, high permeability, high strength, and low losses, making them suitable for high-temperature applications such as magnetic bearing and turbine engine components. There are several investigations on the mechanical, structural, and magnetic properties aiming to explain the unique characteristics of the Fe-Co system [4–7]. Recent theoretical studies performed at static conditions [8–11] showed that the effect of Co on the elasticity of Fe is quite small and thus cannot account for the observed outstanding high-temperature properties. On the other hand, the thermomagnetic effects were reported to have a decisive role on the elasticity of Fe and Fe-Cr [3,12,13]. Considering that a small amount of Co alloying has the ability to enhance the magnetic moment and the Curie temperature (T_C) of Fe, one may anticipate a large magneto-chemical-mechanical coupling in Fe-Co system at elevated temperatures.

According to the equilibrium phase diagram [14], the equimolar Fe-Co system forms a bcc solid solution below ~ 1258 K and transforms to the ordered B2 phase below ~ 1003 K. In Fe-rich alloys, the above temperatures drop below ~ 1183 K and room temperature, respectively. Here we are primarily interested in the high-temperature part of the phase diagram, and thus model the $\text{Fe}_{1-c}\text{Co}_c$ alloys with $c \leq 0.2$ as a bcc solid solution. The temperature dependence

of the cubic elastic constants C_{ij} is described by taking into account the electronic temperature, volume expansion, and magnetic contributions. The first term was shown to be small compared to the others [13] and thus it is omitted.

In order to mimic the magnetic transition near the Curie temperature, we adopt a partial disordered local moment (PDLM) approach. Within PDLM, the magnetic state of $\text{Fe}_{1-c}\text{Co}_c$ is described by a quaternary alloy $(\text{Fe}_{1-x}^{\uparrow}\text{Fe}_x^{\downarrow})_{1-c}(\text{Co}_{1-y}^{\uparrow}\text{Co}_y^{\downarrow})_c$, where x and y stand for the relative fraction of Fe and Co, respectively, possessing opposite spin orientations. PDLM reduces to the ferromagnetic state for $x = y = 0$ and to the disordered local magnetic moment (paramagnetic) state for $x = y = 0.5$. The latter was shown to properly account for the loss of the net magnetization well above T_C [15].

First, for each binary $\text{Fe}_{1-c}\text{Co}_c$ system, we determine the equilibrium lattice constant $a(x,y)$ and the magnetization $\mu(x,y)$ as a function of x and y ($0 \leq x,y \leq 0.5$). Next, according to the empirical expression for the relative magnetization $[\mu(T)/\mu(0)]$ versus relative temperature (T/T_C) [16], we establish the $T(x,y)$ relationship. However, the two degrees of freedom (x,y) gives multiple solutions for $\mu(x,y) = \mu(T)$ [with $\mu(0) = \mu(0,0)$]. For instance, for $\text{Fe}_{0.9}\text{Co}_{0.1}$ the net magnetization of $2.04\mu_B$ obtained for $x = y = 0.05$ (corresponding to ~ 800 K) can also be reached with $x \approx 0.054$ and $y = 0$. The latter configuration has ~ 0.2 mRy/atom smaller energy increase (relative to the ferromagnetic state) than the prior one. In other words, it is easier to induce PDLM moments on the Fe sublattice than on the Co sublattice. Searching for the lowest energy is a possibility to define a unique solution for $\mu(x,y) = \mu(T)$. However, for the present purpose, a constrained-PDLM (c-PDLM) scheme defined as $x = y$ turned out to have the sufficient accuracy [17]. The temperature and concentration dependent lattice parameter $a(c,T)$ is then obtained from $a(x,x)$ using the experimental linear thermal expansion coefficient [18]. The single-crystal elastic constants $C_{ij}(c,T)$ and the corresponding polycrystalline elastic moduli are calculated at $a(c,T)$ using the standard methodology in combination with the above c-PDLM approach. In these calculations we assume that x remains constant with the lattice distortions.

*Corresponding authors: hualei@mail.xjtu.edu.cn; leveute@kth.se

The *ab initio* calculations were performed employing density functional theory within the Perdew-Burke-Ernzerhof generalized gradient approximation [19]. The Kohn-Sham equations were solved using the exact muffin-tin orbitals method based on the Green's function formalism [20] and adopting the scalar-relativistic approximation and the soft-core scheme. The total energy was calculated using the full charge density technique [20]. The substitutional and magnetic disorder was treated within the coherent-potential approximation (CPA) [21]. The Green's function was calculated for 16 complex energy points distributed exponentially on a semicircular contour containing the valence states below the Fermi level. In the basis set we included *s*, *p*, *d*, and *f* orbitals. We used 20 000–25 000 uniformly distributed *k* points in the irreducible wedge of the orthorhombic and monoclinic Brillouin zones. The electrostatic correction to the single-site approximation was described using the screened impurity model [22] with screening parameter 0.6.

The Curie temperatures of Fe and its alloys were derived using the effective Heisenberg Hamiltonian of classical spins \mathbf{e}_i , $H = -1/2 \sum_{i \neq j} J_{ij} \mathbf{e}_i \cdot \mathbf{e}_j$ [23]. The pair exchange interaction parameters J_{ij} were computed from the magnetic force theorem [24]. The critical temperatures were determined from the crossing point of the fourth order Binder cumulant [25] by employing Monte Carlo simulations with the UppAsd program package [26]. Pair interactions of the first 16 coordination shells were included in the simulations where the largest simulation box was $30 \times 30 \times 30$ in terms of bcc unit cell. The calculated Curie temperatures for a few selected systems are listed in Table I. The present concentration dependence $T_C(c)$ is very close to the one predicted by a Korringa-Kohn-Rostoker study [27].

Taking the bulk (*B*), shear (*G*), and Young's (*E*) moduli of pure Fe at 0 K as reference, in Fig. 1 we display the calculated changes (in percent) in the polycrystalline elastic moduli of $\text{Fe}_{1-c}\text{Co}_c$ as a function of Co concentration and temperature. We find that all elastic moduli decrease with increasing temperature. In pure Fe, this decrease is $\gtrsim 30\%$, in line with the experimental [28,29] and former theoretical [3,13] results. In concentrated alloys, the temperature effect is reduced to $\sim 20\%$.

At low temperature, Co doping up to ~ 10 at.% has a small negative impact on the elastic moduli of Fe. These findings confirm the previous theoretical predictions obtained at static

TABLE I. Theoretical equilibrium lattice parameter a (Å), Curie temperature T_C (K), bulk modulus B , shear modulus G , and Young's modulus E (GPa) for ferromagnetic (FM) and paramagnetic (PM) bcc Fe and $\text{Fe}_{0.9}\text{Co}_{0.1}$ alloy calculated at 0 and 1200 K. For comparison, the available experimental data are also shown.

	T	a	T_C	B	G	E
FM Fe	0	2.836	1066	193.9	94.1	243.0
Expt. [28]	4	2.867	1044	173.1	86.9	223.4
FM $\text{Fe}_{0.9}\text{Co}_{0.1}$	0	2.848	1290	179.2	92.6	237.0
PM Fe	0	2.835		170.2	64.2	171.1
PM Fe	1200	2.884		129.7	57.7	150.7
Expt. [29]	1173	2.904		131.1	46.2	124.0

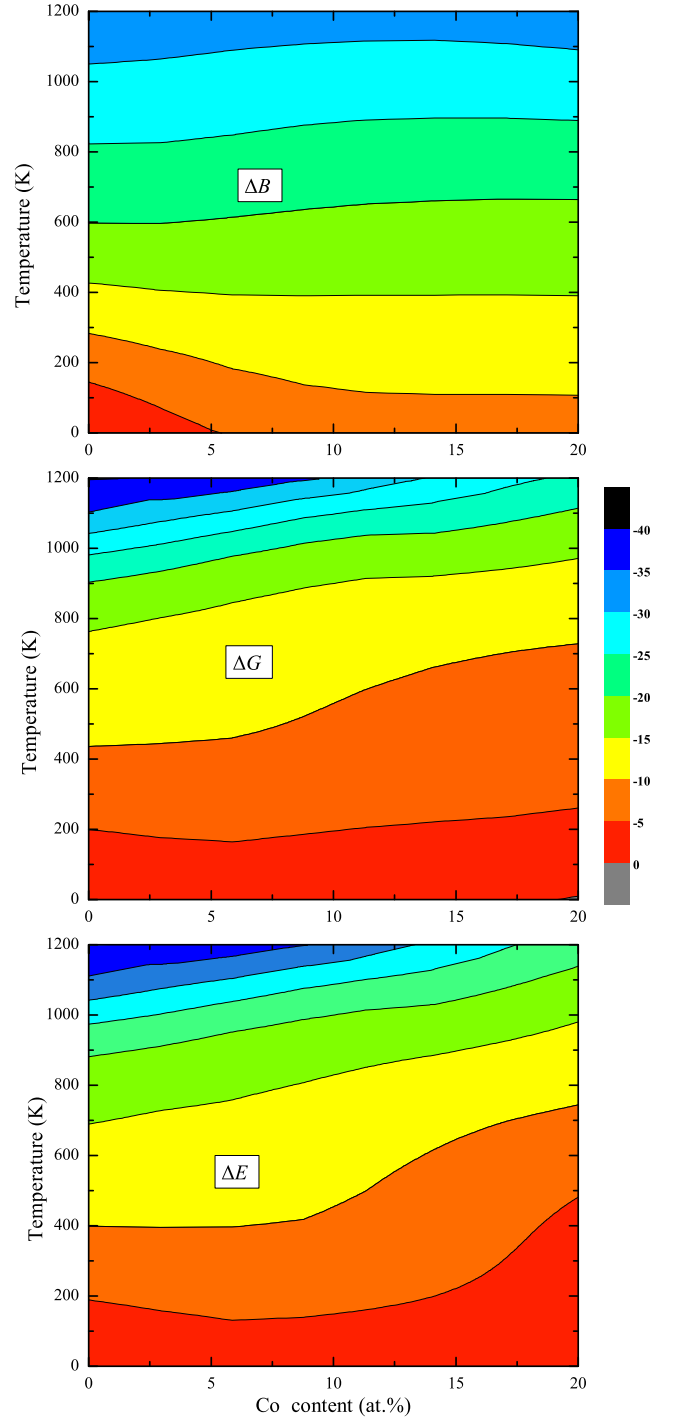


FIG. 1. (Color online) Changes (in %) of the bulk (upper panel), shear (middle panel) and Young's (lower panel) moduli of Fe-Co relative to those of pure Fe at 0 K as a function of temperature and Co concentration.

conditions for ferromagnetic [9] and paramagnetic [11] bcc $\text{Fe}_{1-c}\text{Co}_c$ alloys with $c \leq 0.1$. However, with increasing temperature, alloying exhibits completely different trends. The bulk modulus turns insensitive to Co doping between ~ 400 and 600 K and shows a weak positive slope at larger temperatures. The shear and Young's moduli, on the other hand, become very sensitive to Co alloying as the temperature rises above ~ 800 K.

In particular, at 1000 K, 20 at.% Co increases the shear and Young's moduli by $\gtrsim 10\%$. Around the Curie temperature of Fe, the increment of G and E with Co addition is more than two times larger than that of B .

In Table I we list the theoretical equilibrium lattice parameter, bulk, shear, and Young's moduli of ferromagnetic (FM) and paramagnetic (PM) bcc Fe and $\text{Fe}_{0.9}\text{Co}_{0.1}$ at 0 and 1200 K. At 0 K, 10 at.% Co changes a , B , G , and E by 0.4%, -7.6% , -1.6% , and -2.5% , respectively. Compared to these chemical effects calculated at 0 K, much larger changes occur when going from the long-range FM order to the disordered PM state. Namely, the loss of the net magnetization reduces B , G , and E of Fe by -12.2% , -31.8% , and -29.6% , respectively. Combining magnetism with thermal expansion further decreases the elastic moduli relative to those of PM Fe computed at 0 K. Based on the above figures, one concludes that magnetism produces by far the most significant changes in the elasticity of the Fe-Co system.

To understand the reason behind the anomalous alloying-induced variations of the shear and Young's moduli at high temperature, we consider the composition and temperature dependence of the single-crystal elastic constants of Fe-Co alloys. At low temperatures, tetragonal shear elastic constant $C' = (C_{11} - C_{12})/2$ (Fig. 2, upper panel) is slightly decreased by Co addition (-0.5 GPa per at.% Co, for $c \lesssim 0.15$), which has previously been attributed to the volume expansion effect [8]. Similar (-0.3 GPa per at.% Co) alloying effect was reported also for the paramagnetic state [11]. On the other hand, for all alloys C' is found to strongly decrease as a function of temperature. At 1200 K, the maximum change of C' is around -70% compared to pure Fe at 0 K. However, this change becomes $+137\%$ when compared to pure Fe at 1200 K. This is a very large alloying effect especially if we consider the nearly vanishing impact of Co on C' of Fe at 0 K. The trend of the orthorhombic shear elastic constant C_{44} of Fe-Co alloys (not shown) is different from that of C' . Nevertheless, the largest change for C_{44} (12%) is calculated to remain far below that for C' making the tetragonal shear elastic constant primary responsible for the variations of G and E .

The strong negative effect of temperature on C' is connected to the particular electronic structure of Fe. In prototypical (non-magnetic, NM) bcc metals with mostly t_{2g} states populated (having d occupation number N^d approximately between 3 and 5) the bonds are directed towards the cube corners [30], and the band energy contribution to C' shows a maximum value [12,31]. This situation corresponds to the deep valley in the density of states of NM Fe (Fig. 3 upper panel). Increasing the number of d electrons fills up the e_g states as well, creating weakly directional bonds and reducing substantially the band energy term in C' (with a minimum at $N^d \approx 7$, Ref. [12]). In FM Fe (Fig. 3 middle panel), the minority spin channel shows typical bcc behavior ($2N_{\downarrow}^d \approx 4.3$) giving rise to large positive "spin-projected" C'_{\uparrow} , whereas the majority spin channel is nearly fully occupied ($2N_{\uparrow}^d \approx 8.8$) yielding small C'_{\downarrow} . It is primarily the minority channel showing mostly t_{2g} character that stabilizes FM Fe mechanically. In PM Fe, on the other hand, in both spin channels (they are equivalent) the d electrons are more homogeneously distributed between the e_g and t_{2g} states (Fig. 3 lower panel). Furthermore, the PM e_g and t_{2g}

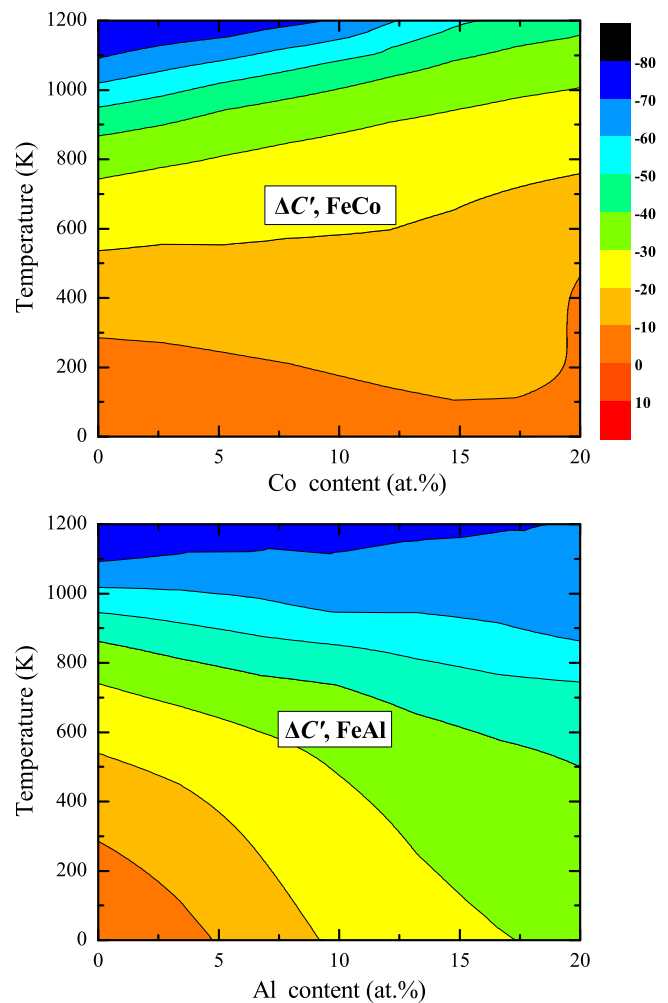


FIG. 2. (Color online) Changes (in %) of the tetragonal shear elastic constant C' of Fe-Co and Fe-Al relative to those of pure Fe at 0 K as a function of temperature and Co and Al concentration.

states have similar weights near the Fermi level (E_F). This is in contrast to FM (NM) Fe, for which the e_g state have a very small (large) weight at E_F . Due to the persisting local exchange splitting (DLM state), however, there is still a local minimum in the PM e_g band at E_F , which weakly stabilizes dynamically the PM state as opposite to the NM state.

We suggest that the anomalous behavior of C' of Fe-Co around and slightly beyond the Curie temperature of Fe as a function of Co content is the consequence of the small intrinsic alloying effects in combination with the increased magnetic transition temperature. Cobalt addition to Fe leads to increased T_C as compared to that of pure Fe (Table I), which has been explained in terms of electronic structure [27]. The primary effect of Co doping on Fe is filling up the majority spin channel leaving the minority channel almost intact. Therefore, to a large extent the above-discussed scenario for the temperature-induced magnetoelastic softening remains valid for the Fe-rich Fe-Co alloys as well. Now, since Co raises the critical temperature of Fe, it shifts the magnetoelastic softening experienced in pure Fe to larger temperatures. That is why the contour lines in Figs. 1 and 2 (upper panel) have marked positive slopes at high temperatures. These slopes will

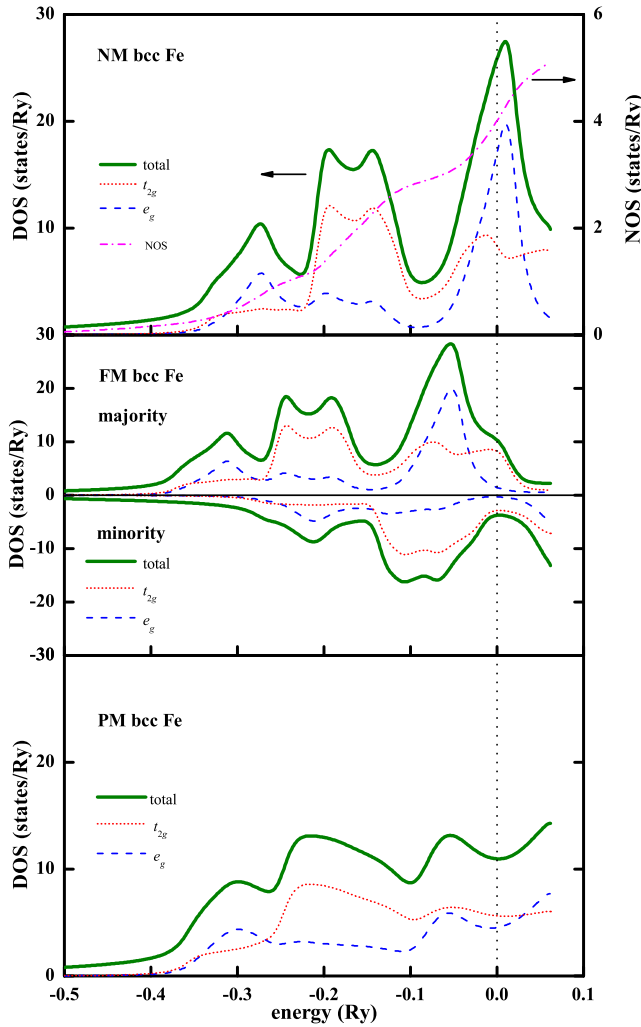


FIG. 3. (Color online) Total and partial (e_g and t_{2g}) density of states of nonmagnetic (NM, upper panel), ferromagnetic (FM, middle panel), and paramagnetic (PM, lower panel) Fe in the bcc lattice. The dashed lines mark the Fermi level E_F . For NM, the occupation number is shown on the right axis. For NM and PM, only one spin channel is shown.

eventually flatten when the temperature rises beyond the Curie point of the alloy.

Based on the above findings, one might naively expect that, in general, alloying elements which keep the bcc phase stable

but decrease/increase the Curie point of Fe should produce an elastic softening/hardening at elevated temperatures. However, the actual elastic softening/hardening also depends on the intrinsic alloying effects. In the case of Co doping, alloying has small influence on the static elastic parameters of Fe, but that is not always the case [8,11]. Figure 2 (lower panel) shows the tetragonal shear elastic constant of Fe-Al as a function of Al content and temperature. In ferromagnetic Fe at 0 K, 10% Al addition decreases (increases) C' (C_{44} , not shown) by $\sim 22\%$ ($\sim 11\%$). In paramagnetic Fe, 10% Al gives $\sim 29\%$ ($\sim 4\%$) increase for C' (C_{44}). Assuming constant T_C with composition, one may reasonably estimate that alloying effects in C' of Fe-Al should vanish somewhere around the Curie point. Indeed, at small Al content, the contour lines are nearly parallel with the x axis in the lower panel of Fig. 2. However, in Fe-rich Fe-Al alloys, T_C decreases by ~ 6 K per at.% Al. This feature is nicely reflected by the broadening of the “constant” C' region with increasing Al concentration. The above small influence of Al on C' should eventually be present also in the shear and Young’s moduli of the Fe-Al system within this temperature interval. Experimental verification of this phenomenon is encouraged.

The elasticity of bcc Fe strongly depends on its magnetic state, which in turn is very sensitive to the temperature and alloying. Here we have demonstrated that adding a small amount of Co or Al to Fe produces complex trends in the thermophysical parameters. Namely, the low-temperature regime (far below the magnetic transition temperature) is governed by the chemical effects, which are relative small for Co but substantial for Al. However, at high temperatures, Co (Al) proves to be a rather strong (weak) alloying agent. Cobalt substantially enhances the tetragonal shear elastic constant of Fe and by that also the polycrystalline elastic moduli. The unique elastic hardening effect of Co has a clear magnetic origin connected with the small intrinsic alloying effects and the pronounced change of the Curie temperature.

The National Science Foundation of China (No. 51301126), the National Basic Research Program of China (No. 2014CB644003 and No. 2012CB619402), the Scientific Research Foundation for the Returned Overseas Chinese Scholars, the Swedish Research Council, the Swedish Steel Producers’ Association, the European Research Council, and the Hungarian Scientific Research Fund (OTKA 84078 and 109570) are acknowledged for financial support.

[1] H. L. Skriver, *Phys. Rev. B* **31**, 1909 (1985).
 [2] I. Leonov, A. I. Poteryaev, V. I. Anisimov, and D. Vollhardt, *Phys. Rev. Lett.* **106**, 106405 (2011).
 [3] H. L. Zhang, B. Johansson, and L. Vitos, *Phys. Rev. B* **84**, 140411(R) (2011).
 [4] M. S. Lataifeh, *J. Phys. Soc. Jpn.* **69**, 248 (2000).
 [5] T. Sourmail, *Prog. Mater. Sci.* **50**, 816 (2005).
 [6] B. Warot-Fonrose, C. Gatel, L. Calmels, V. Serin, E. Snoeck, and S. Cherifi, *J. Appl. Phys.* **107**, 09D301 (2010).

[7] S. Khmelevskiy and P. Mohn, *Phys. Rev. B* **69**, 140404(R) (2004).
 [8] H. L. Zhang, M. P. J. Punkkinen, B. Johansson, S. Hertzman, and L. Vitos, *Phys. Rev. B* **81**, 184105 (2010).
 [9] H. L. Zhang, M. P. J. Punkkinen, B. Johansson, and L. Vitos, *J. Phys.: Condens. Matter* **22**, 275402 (2010).
 [10] H. L. Zhang, N. Al-Zoubi, B. Johansson, and L. Vitos, *J. Appl. Phys.* **110**, 073707 (2011).
 [11] H. L. Zhang, M. P. J. Punkkinen, B. Johansson, and L. Vitos, *Phys. Rev. B* **85**, 054107 (2012).

- [12] H. Hasegawa, M. W. Finnis, and D. G. Pettifor, *J. Phys. F: Met. Phys.* **15**, 19 (1985).
- [13] V. I. Razumovskiy, A. V. Ruban, and P. A. Korzhavyi, *Phys. Rev. Lett.* **107**, 205504 (2011).
- [14] O. Kubaschewski, *Iron-Binary Phase Diagrams* (Springer, Berlin, 1982).
- [15] B. L. Györfy, A. J. Pindor, G. M. Stocks, J. Staunton, and H. Winter, *J. Phys. F: Met. Phys.* **15**, 1337 (1985).
- [16] M. D. Kuz'min, *Phys. Rev. Lett.* **94**, 107204 (2005).
- [17] We have estimated the effect of going from the (0.05,0.05) PDLM state [i.e., $(\text{Fe}_{0.95}^{\uparrow}\text{Fe}_{0.05}^{\downarrow})_{0.9}(\text{Co}_{0.95}^{\uparrow}\text{Co}_{0.05}^{\downarrow})_{0.1}$] to the (0.054,0.0) PDLM state [i.e., $(\text{Fe}_{0.946}^{\uparrow}\text{Fe}_{0.054}^{\downarrow})_{0.9}\text{Co}_{0.1}^{\uparrow}$] by computing the equilibrium bulk properties for these two alloys. The results show that the differences between the two-dimensional PDLM and the constrained PDLM (c-PDLM) are $\lesssim 10^{-4}$ Å for the lattice parameter and $\lesssim 1$ GPa for the elastic parameters. These effects are far below the variations induced by alloying or temperature.
- [18] Z. S. Basinski, W. Hume-Rothery, and A. L. Sutton, *Proc. R. Soc. London Ser. A* **229**, 459 (1955).
- [19] J. P. Perdew, K. Burke, and M. Ernzerhof, *Phys. Rev. Lett.* **77**, 3865 (1996).
- [20] L. Vitos, *Phys. Rev. B* **64**, 014107 (2001).
- [21] L. Vitos, I. A. Abrikosov, and B. Johansson, *Phys. Rev. Lett.* **87**, 156401 (2001).
- [22] P. A. Korzhavyi, A. V. Ruban, I. A. Abrikosov, and H. L. Skriver, *Phys. Rev. B* **51**, 5773 (1995).
- [23] I. Turek, J. Kudrnovský, V. Drchal, and P. Bruno, *Philos. Mag.* **86**, 1713 (2006).
- [24] A. I. Liechtenstein, M. I. Katsnelson, and V. A. Gubanov, *J. Phys. F: Met. Phys.* **14**, L125 (1984).
- [25] D. Landau and K. Binder, *Guide to Monte Carlo Simulations in Statistical Physics* (Cambridge University Press, Cambridge, 2000).
- [26] B. Skubic, J. Hellsvik, L. Nordström, and O. Eriksson, *J. Phys.: Condens. Matter* **20**, 315203 (2008).
- [27] M. Lezaic, P. Mavropoulos, and S. Blügel, *Appl. Phys. Lett.* **90**, 082504 (2007).
- [28] J. A. Rayne and B. S. Chandrasekhar, *Phys. Rev.* **122**, 1714 (1961).
- [29] D. J. Dever, *J. Appl. Phys.* **43**, 3293 (1972).
- [30] T. E. Jones, M. E. Eberhart, and D. P. Clougherty, *Phys. Rev. Lett.* **100**, 017208 (2008).
- [31] M. W. Finnis, K. L. Kear, and D. G. Pettifor, *Phys. Rev. Lett.* **52**, 291 (1984).